Signal Quality Assessment of Retinal Optical Coherence Tomography Images

Yijun Huang,[1] *Sapna Gangaputra,*[1] *Kristine E. Lee,*[2] *Ashwini R. Narkar,*[1] *Ronald Klein,*[2] *Barbara E. K. Klein,*[2] *Stacy M. Meuer,*[2] *and Ronald P. Danis*[1]

Purpose. The purpose of this article was to assess signal quality of retinal optical coherence tomography (OCT) images from multiple devices using subjective and quantitative measurements.

Methods. A total of 120 multiframe OCT images from 4 spectral domain OCT devices (Cirrus, RTVue, Spectralis, and 3D OCT-1000) were evaluated subjectively by trained graders, and measured quantitatively using a derived parameter, maximum tissue contrast index (mTCI). An intensity histogram decomposition model was proposed to separate the foreground and background information of OCT images and to calculate the mTCI. The mTCI results were compared with the manufacturer signal index (MSI) provided by the respective devices, and to the subjective grading scores (SGS).

Results. Statistically significant correlations were observed between the paired methods (i.e., SGS and MSI, SGS and mTCI, and mTCI and MSI). Fisher's Z transformation indicated the Pearson correlation coefficient $\rho \geq 0.8$ for all devices. Using the Deming regression, correlation parameters between the paired methods were established. This allowed conversion from the proprietary MSI values to SGS and mTCI that are universally applied to each device.

Conclusions. The study suggests signal quality of retinal OCT images can be evaluated subjectively and objectively, independent of the devices. Together with the proposed histogram decomposition model, mTCI may be used as a standardization metric for OCT signal quality that would affect measurements. (*Invest Ophthalmol Vis Sci.* 2012;53:2133–2141) DOI:10.1167/iovs.11-8755

The recent introduction of spectral domain detection techniques has made optical coherence tomography (OCT) an increasingly useful clinical tool for providing valuable diagnostic information on retinal structure.[1,2] Multiple manufacturers have developed spectral domain OCT devices with automatic software packages for visualizing OCT images, calculating signal quality and other image-related parameters, delineating boundaries of the retinal layers, and analyzing thickness and volume of the retina. Although these software tools provide tremendous convenience in a busy clinical environment, most of them are proprietary in nature and as a result it is challenging to compare OCT images and results from different devices.[3,4] The lack of standardization of OCT data and measurement results make it problematic for multicenter clinical studies to centrally analyze images collected from various devices.

Many devices provide quantitative parameters to estimate the signal quality of OCT images; we collectively refer to these parameters as the manufacturer signal index (MSI) in this study. The MSI parameters are not only useful for providing immediate feedback of signal quality to users during data acquisition, but they are also found to be important determinants of automated tissue layer segmentation accuracy. Several studies in time domain[5–8] and spectral domain[9,10] OCTs reported correlation between MSI values with retinal nerve fiber layer and retinal thickness measurements. In addition, manufacturers usually recommend a threshold for their MSI values, below which the automatic measurement results may not be reliable. On the other hand, because each manufacturer developed its own approach, the underlying algorithm, the range, the threshold recommendation, and even the naming convention are different from one device to another (Table 1). There is a need for standardization for OCT signal quality measurement when multiple OCT devices are involved in clinical trials.

The present study was designed to explore what is common among spectral domain OCT images and to develop subjective and quantitative methods for signal quality measurements. We developed a grading protocol for subjective assessment. For quantitative assessment, we propose an intensity histogram decomposition model and derive a quantitative parameter, the maximum tissue contrast index (mTCI). These methods were applied to an OCT image dataset selected from several spectral domain OCT devices and compared with their corresponding MSI values.

Methods

Data Collection

This is a retrospective study using OCT images selected from a large database at the Fundus Photograph Reading Center, University of Wisconsin, collected from various clinical trials. The study evaluated images obtained from four spectral domain OCT devices: Cirrus (Carl Zeiss Meditec, Inc., Dublin, CA), RTVue (Optovue, Inc., Fremont, CA), Spectralis (Heidelberg Engineering, Inc., Heidelberg, Germany), and 3D OCT-1000 (Topcon, Inc., Tokyo, Japan). These spectral domain

From the [1]Fundus Photograph Reading Center, and [2]Ocular Epidemiology Reading Center, Department of Ophthalmology, University of Wisconsin-Madison, Madison, Wisconsin.

Supported in part by an unrestricted grant from Research to Prevent Blindness, New York, New York, to the Department of Ophthalmology and Visual Sciences, University of Wisconsin-Madison, and in part by National Institutes of Health grant EY06594 (RK and BEKK). The content is solely the responsibility of the authors and does not necessarily reflect the official views of the National Eye Institute or the National Institutes of Health.

Submitted for publication October 6, 2011; revised January 17, 2012; accepted February 19, 2012.

Disclosure: **R. Klein**, Topcon Inc. (R); **Y. Huang**, None; **S. Gangaputra**, None; **K.E. Lee**, None; **A.R. Narkar**, None; **B.E.K. Klein**, None; **S.M. Meuer**, None; **R.P Danis**, None

Corresponding author: Yijun Huang, Fundus Photograph Reading Center, Department of Ophthalmology, University of Wisconsin-Madison, 8010 Excelsior Dr, Ste 100, Madison, WI 53717; yhuang@rc.ophth.wisc.edu.

Table 1. List of the OCT Devices, Software Version, Name, Range, Threshold Recommendation of the MSI, and Descriptive MSI Statistics for the Data Samples Used in This Study

	Device			
	Cirrus	**RTVue**	**Spectralis**	**3D OCT-1000**
Company	Carl Zeiss Meditec, Inc., Dublin, CA	Optovue, Inc., Freemont, CA	Heidelberg Engineering, Inc., Heidelberg, Germany	Topcon, Inc., Tokyo, Japan
Software version	research browser 5.0.0.326	UWFPRC 4.0.6.13	5.1.3	4.13.002.02*
MSI name	Signal strength	Signal strength index	Quality	Image quality metric
Range	0–10	0–100	0–40	0–100
Recommended Threshold	6	39	15	45
MSI statistics for this study				
N	30	30	30	30
Minimum	0	17.6	7.6	15.28
Maximum	10	73	32	74.76
Mean	5.70	47.26	21.24	41.09
Range tested	0–10	15–80	5-35	10–80
K-S test	0.2000	0.1933	0.1983	0.1548

The Kolmogorov-Smirnov (K-S) test was used to examine distribution uniformity of the data samples on the tested MSI ranges.
* All 3D OCT-1000 scans were captured with software version 2.12.

OCT devices were chosen because they included MSI information in their operation manuals.

For each device, 30 samples of multiframe OCT images were selected to cover the spectrum of varying signal quality from poor to excellent. All images were macular volume ("cube") scans covering a 20° x 20° region centered at the fovea, and had different sampling density and averaging schemes: Cirrus, 512 × 128 (512 A-scans per frame, 128 frames), without averaging or "overlapping"; RTVue, 512 × 128, without averaging; Spectralis, 512 × 97, automatic real-time (ART) averaging of 5 frames; and 3D-OCT 1000, 512 × 128, without averaging. Image samples included scans from normal and diseased retina: 60 (50.0%) are from eyes with age-related macular degeneration, 32 (26.7%) are from diabetic retinopathy, 18 (15.0%) are from retinal vein occlusion, and 10 (8.3%) are from other disease types and normal retinas. Although lesion appearances in OCT images were not investigated in this study, the following retinal abnormalities were observed: epiretinal membrane (15 occurrences), posterior vitreous detachment (7), cyst (45), diffuse macular edema (7), subretinal fluid (30), drusen (21), pigment epithelium detachment (1), choroidal neovascularization (34), and geographic atrophy (3).

The study was conducted in accordance with Health Insurance Portability and Accountability Act (HIPAA) requirements and the tenets of the Declaration of Helsinki. All images were de-identified of patient health information, and the study protocol was approved by the institutional review board of the University of Wisconsin-Madison.

Subjective Signal Quality Grading Procedure

OCT images were evaluated independently by three trained graders using a subjective grading scheme. Graders were required to make a binary decision (yes/no) on the following nine questions ranked according to the ascending signal quality from poor to excellent (Fig. 1):

(1) Difference in reflectivity between the outer retino-choroidal complex and vitreous
(2) Visibility of the vitreo-retinal interface
(3) Difference in reflectivity between retinal nerve fiber layer and vitreous
(4) Difference in reflectivity between plexiform layer and vitreous
(5) Visibility of multiple layers within the outer retino-choroidal complex
(6) Visibility of the ganglion cell layer
(7) Difference in reflectivity between outer nuclear layer and vitreous
(8) Visibility of external limiting membrane
(9) Visibility of choroidal/scleral interface

For the subjective grading score (SGS), 1 point was scored for each question answered yes and 0 to question answered no. The scores were added up for each grader and the SGS, ranging from 0 to 9, was the mean value of the cumulative scores from the three graders.

All grading was performed using the corresponding manufacturer review software (Table 1). OCT images were shown in gray-scale format and used the largest screen size allowable by the review software. Graders were masked to the MSI values, and were requested to make an overall assessment based on all frames of the multiframe image. In addition, graders were trained through a training data set consisting of 15 randomly selected images from each device, before the actual grading.

Quantitative Assessment

Manufacturer Signal Index. The MSI values were assigned by each device. Cirrus, RTVue, and 3D OCT-1000 assigned a single MSI value per multiframe image; we recorded the MSI values directly from the respective review software. In Spectralis, MSI value was assigned per frame. We extracted MSI from each frame and calculated the average MSI for the multiframe image.

Maximum Tissue Contrast Index. OCT scans were exported from the respective manufacturer software in raw format and analyzed using a custom-developed MATLAB program (Mathworks, Natick, MA). Procedures of exporting raw pixel values were similar to those used by other research groups,[10] and the data were saved in single (float) precision in MATLAB. Histogram plots were obtained by binning the pixel intensity into 512 steps of equal distance across the data range.

mTCI values were calculated based on the entire multiframe OCT image. The detailed algorithm to derive mTCI is described in the Appendix. In brief, mTCI was designed as a ratio of the signal intensity between the foreground and the background, based on the histogram characteristics of the OCT images. mTCI value can be interpreted as a signal-to-noise ratio measurement, where a score of 1 (the lower limit) indicates the signal and noise are indistinguishable and higher values indicates better quality. There is no upper limit for mTCI.

Statistical Analysis

Descriptive statistics were performed on the MSI of the data samples from each device. The Kolmogorov-Smirnov (K-S) test was used to

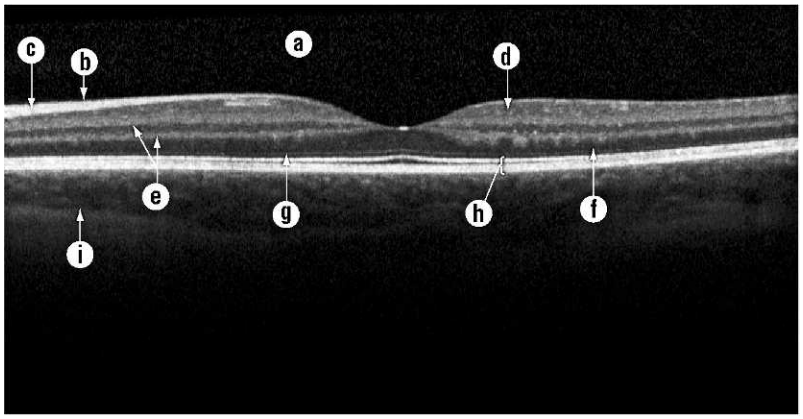

Figure 1. A representative OCT image with subjective grading scheme applied. The graded OCT features were labeled (a) vitreous, (b) vitreo-retinal interface, (c) nerve fiber layer, (d) ganglion cell layer, (e) plexiform layers, (f) outer nuclear layer, (g) outer limiting membrane, (h) outer retino-choroidal complex, (i) choroidal/scleral interface. Question 1 in the subjective grading scheme corresponds to the intensity difference between features a and h; question 2, visibility of b; question 3, intensity difference between a and c; question 4, intensity difference between a and e; question 5, visibility of multiple layers within h; question 6, visibility of d (against c and e); question 7, intensity difference between a and f; question 8, visibility of g; and question 9, visibility of i.

examine if the data sample was uniformly distributed in the tested range for each device.

For subjective grading, graders were paired and weighted kappa test was used to evaluate intergrader agreement. A weight of 0.75 was assigned to one-step disagreement and 0 was assigned to two- or more-step disagreement.

Pearson correlation was used to test the statistical significance when comparing between two signal quality evaluation methods (SGS

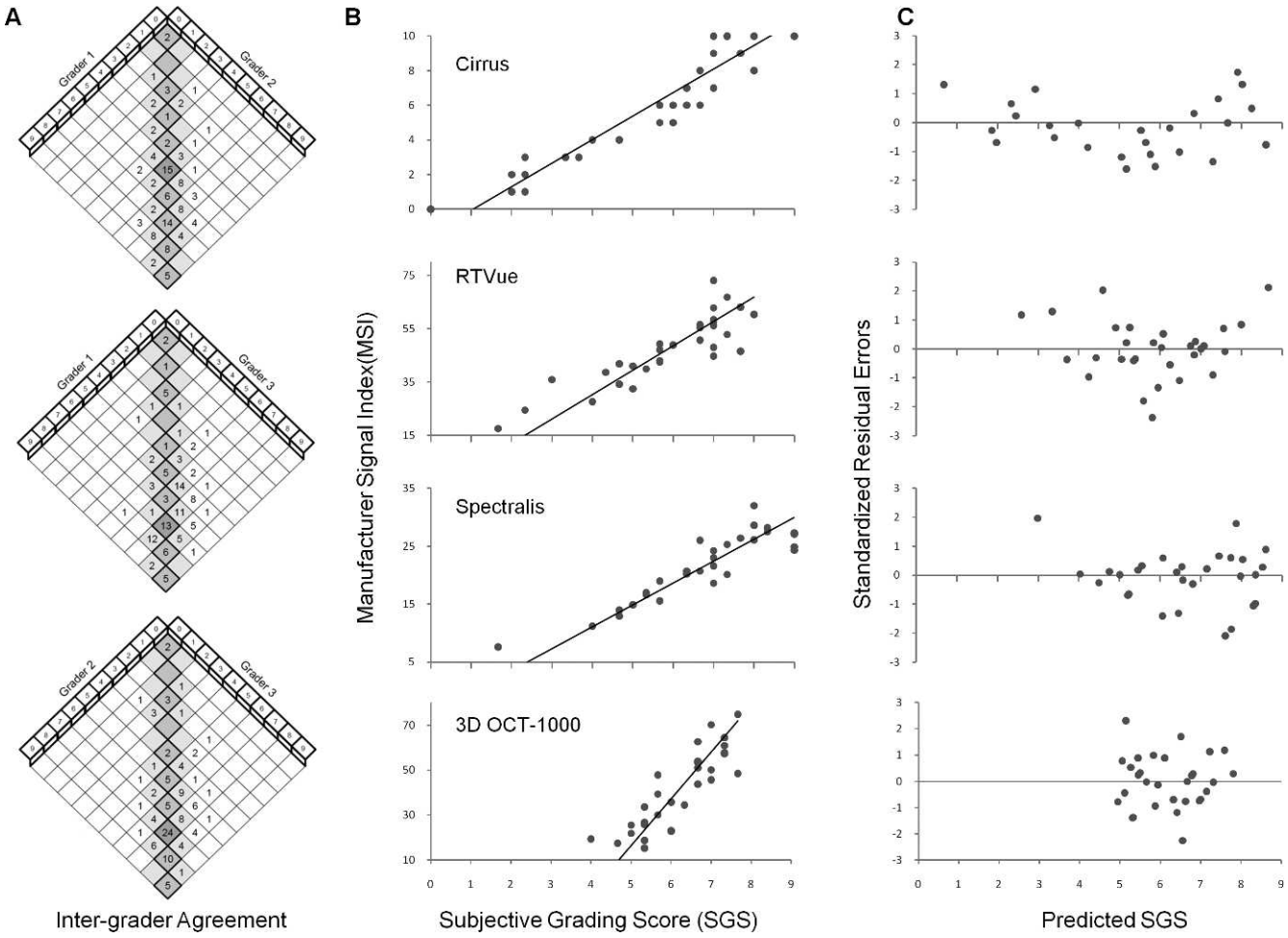

Figure 2. Subjective assessment of OCT signal quality. (**A**) Kappa analysis of intergrader reproducibility of the SGS. (**B**) Scatter plot of the SGS and MSI values. Solid line shows the linear relationship determined by Deming regression. (**C**) Scatter plot of the standardized residual errors and the predicted SGS. The standardized residual errors were the orthogonal distances of all data points from the regression line, normalized by its standard deviation.

versus MSI, mTCI versus MSI, or mTCI versus SGS). One-tail Fisher's Z transformation was used to test if the correlation between the paired methods was at least 0.8.

As Pearson correlation coefficient greater than 0.8 indicated the strength of a linear relationship between the method pairs, it was further assumed that the studied methods linearly approximated the underlying OCT signal quality in their respective range. As each method independently estimated the OCT signal quality, however, it used its own choice of scaling and offset parameters. Deming regression analysis[11] was performed to quantify the relationship between the method pair (i.e., the slope and the intercept of the regression line). Deming regression minimizes the squared deviation of the orthogonal distances of the observed data from the regression line, and is applied in method-comparison analysis when random errors from both methods need to be taken into account. The standardized residual errors were the orthogonal distances of all data points from the regression line, normalized by its standard deviation, and plotted against the predicted values. In addition, 95% confidence intervals of the estimate of the Deming regression parameters (i.e., slope and intercept) were obtained by the Jackknife method, omitting one pair of data at a time to obtain the Deming regression estimates.

Results

A total of 120 multiframe images from 4 spectral domain OCT devices were included in this study. The minimum, maximum, and mean MSI values of the data samples for each device were tabulated (Table 1). It was noted that the selected samples encompassed a large portion, but not the entire range, of the potential MSI values specified by the device manufacturers. The K-S test was performed to ensure the data samples were uniformly distributed within the tested range. The critical value of the K-S test for validating distribution uniformity for a sample size of 30 and with level of significance 0.05 was 0.24. The K-S statistics for all devices were below the critical value, indicating the data samples followed uniform distribution.

Subjective Grading

Subjective assessment by OCT graders showed fair-to-good agreements between graders (Fig. 2A). Among all 360 observations, 153 (42.5%) were in exact agreement, 301 (83.6%) were within one step, and 352 (97.8%) were within two steps. There was no case when the difference between any two graders was more than three steps. The mean value of the pair-wise weighted Kappa was 0.57.

Pearson correlation was performed to evaluate the correlations between the SGS and MSI values. Pearson correlation coefficients yielded significant correlations ($P < 0.0001$), and one-tail Fisher's Z transformation further confirmed correlation coefficient $\rho \geq 0.8$ for all devices. With the assumption that the method pair was linearly correlated, scatter plot and regression line of the Deming regression were shown (Fig. 2B) and the correlation parameters were listed (Table 2). The random error, as estimated by the plot of standardized residual errors versus the predicted SGS (Fig. 2C), indicated the model provided a good fit with no marked pattern or trend. The results suggested that SGS can be used as a common signal quality determinant that was correlated with MSI values from each device.

Quantitative Assessments

The mTCI values were calculated for all images and similar correlation analyses were performed between SGS and mTCI, and between mTCI and MSI, respectively. Pearson correlation indicated the correlation coefficient $\rho \geq 0.8$ ($P < 0.0001$), which suggested linear relationship between mTCI and SGS. Using SGS as the predictor to mTCI, the scatter plot with the

Table 2. Slope, Intercept, and Correlation Coefficients Between Method Pairs of Signal Quality Measurement (x versus y) Using Deming Regression

	SGS versus MSI			SGS versus mTCI			mTCI versus MSI		
Device	**Slope**	**Intercept**	**Correlation Coefficient**	**Slope**	**Intercept**	**Correlation Coefficient**	**Slope**	**Intercept**	**Correlation Coefficient**
Cirrus	1.36	−1.43	0.95	0.64	1.55	0.89	2.14	−4.73	0.91
	(1.16, 1.57)	(−2.55, −0.31)		(0.52, 0.76)	(0.99, 2.10)		(1.68, 2.59)	(−7.03, −2.43)	
RTVue	9.11	−6.06	0.87	0.53	2.38	0.83	15.32	−36.63	0.89
	(6.47, 11.74)	(−21.97, 9.85)		(0.36, 0.70)	(1.36, 3.40)		(12.22, 18.43)	(−54.30, −18.96)	
Spectralis	3.78	−4.02	0.91	2.29	−8.7	0.82	1.79	9.48	0.94
	(2.75, 4.80)	(−10.83, 2.88)		(1.36, 3.21)	(−15.10, −2.30)		(1.51, 2.06)	(7.52, 11.44)	
3D OCT-1000	20.78	−87.49	0.86	0.9	−0.37	0.81	22.07	−73.66	0.88
	(15.94, 25.61)	(−118.59, 56.40)		(0.66, 1.15)	(−1.94, 1.19)		(17.15, 26.98)	(−100.34, −46.98)	

The numbers in parentheses indicate 95% confidence intervals of the estimates.

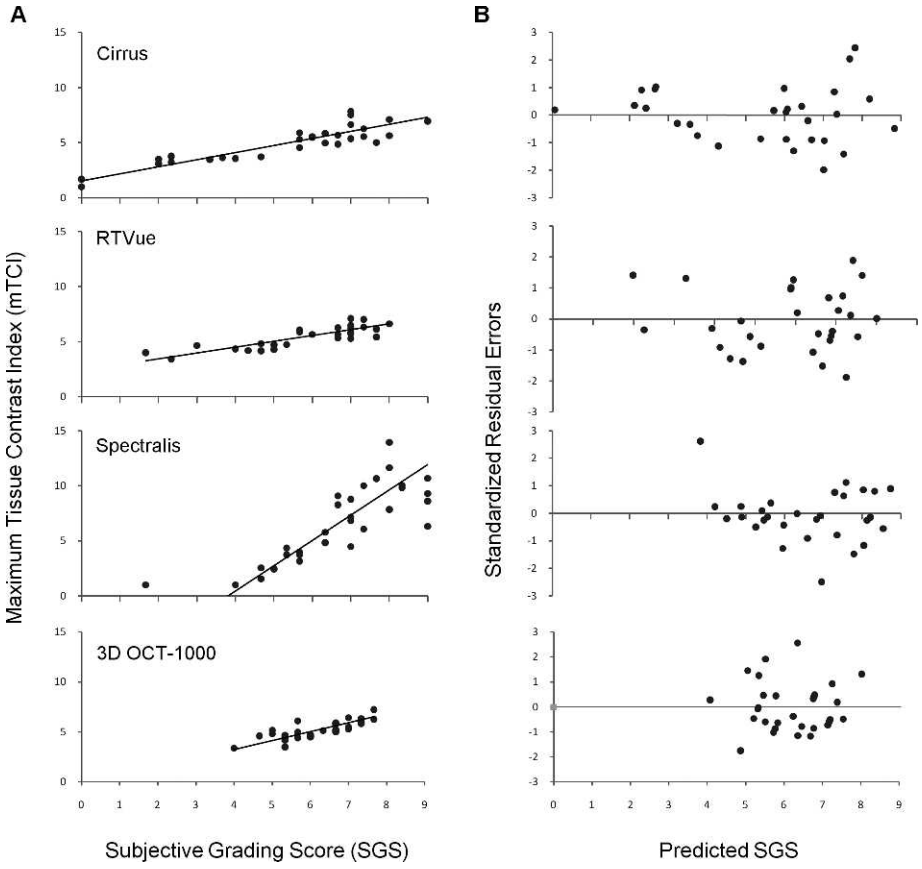

Figure 3. Comparison of the SGS and the mTCI values. (**A**) Scatter plot of the mTCI and SGS values. Solid line shows Deming regression. (**B**) Scatter plot of the standardized residual errors and the predicted SGS.

Deming regression line between mTCI and SGS was depicted (Fig. 3A), and the random error was shown in the standardized residual plot (Fig. 3B). The regression parameters and 95% confidence intervals of the estimates are listed (Table 2). These plots suggested mTCI, another common signal quality determinant that can be obtained quantitatively, was strongly correlated to SGS.

Similarly, relationship between mTCI and MSI was evaluated using mTCI as the predictor. The comparison results yielded similar outcomes (Fig. 4), which suggested mTCI can be used as a quantitative parameter in evaluating OCT signal quality.

Signal Quality Estimates Using Common Determinants

Each of the four spectral domain OCT devices used in this study provided recommendation of a threshold for MSI, and cautioned that the corresponding automatic segmentation algorithm may not work reliably if the MSI value was below the threshold; however, the units and values differed between instruments. For retinal thickness measurement, Cirrus recommended 6, RTVue recommended 39, and 3D OCT-1000 recommended 45. Spectralis recommended 15 as the borderline quality score, not specifically for retinal thickness.

Table 3 lists the SGS and mTCI values corresponding to the recommended MSI thresholds from each device. The corresponding SGS thresholds from each device indicated that the minimum signal quality for images to be considered as acceptable was SGS $\geq$ 5. In addition, the corresponding mTCI thresholds for Cirrus, RTVue, and 3D OCT-1000 were similar, and that for Spectralis was lower, presumably in concordance with the difference in purposes of which the thresholds were chosen.

Discussion

The aim of the study was to evaluate signal quality of OCT images from multiple OCT devices. We hypothesized that the prerequisite for discerning OCT images with good quality as well as for reliable performance of an automated segmentation algorithm was that the targeted features in an OCT image were separable from the background (noise). We developed a subjective grading scheme and a quantitative parameter for this purpose, and our results indicated strong correlation between the SGS and MSI values for each device, as well as strong correlation between the mTCI and MSI values. These findings show that the signal quality of OCT images can be evaluated both subjectively and objectively using approaches that are independent of the OCT devices. In addition, after the correlation coefficients between method pairs are determined, threshold recommendations from each device can be converted to the SGS and mTCI values. The data resulting from these conversions in our study showed the minimum SGS value for an OCT image with acceptable quality is $\geq$ 5. Because the questionnaire was designed to have an ascending order, this was likely associated with the affirmative answers to visualization of the vitreo-retinal interface (question 2) and layered structure of the outer retino-choroidal complex (question 5). When the threshold recommendation was examined in the mTCI scale, the data showed that the recommendations from Cirrus, RTVue, and 3D OCT-1000 were closely matched, whereas the recommendation from Spectralis had a lower

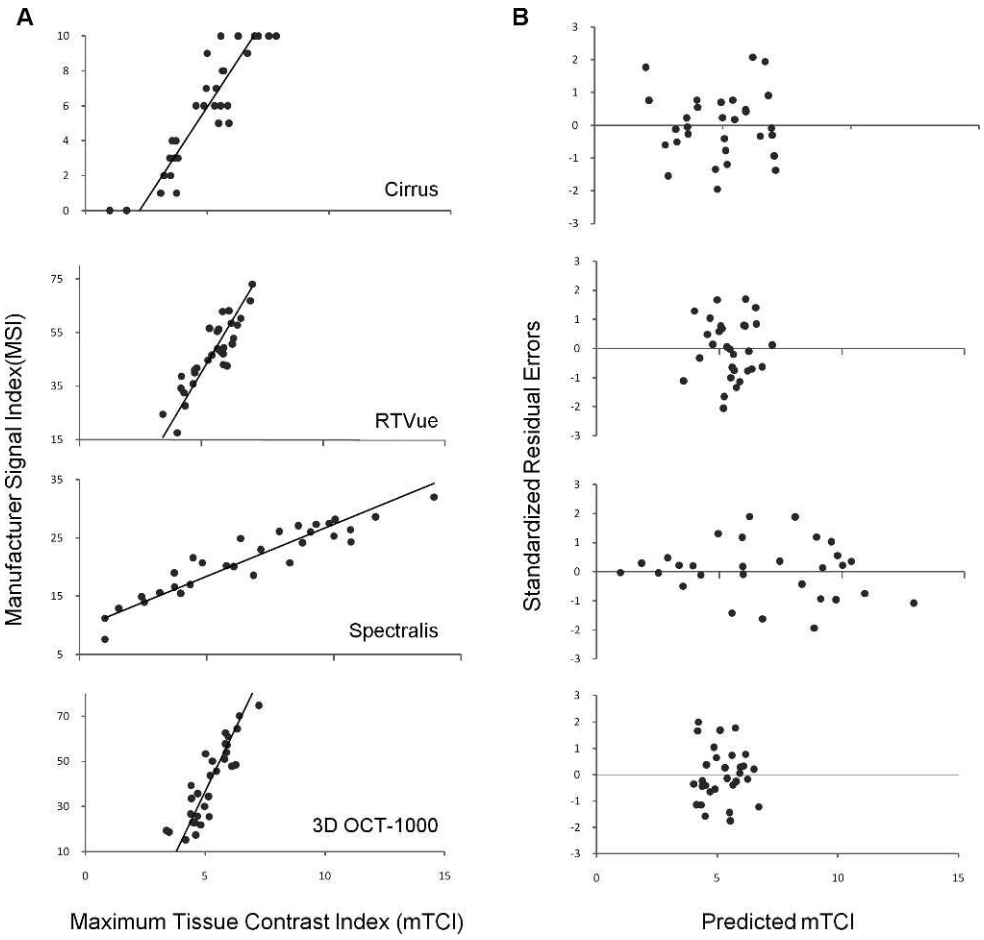

Figure 4. Comparison of quantitative measurement of OCT signal quality using mTCI and MSI. (**A**) Scatter plot of the mTCI and MSI values. Solid line shows Deming regression. (**B**) Scatter plot of the standardized residual errors and the predicted mTCI.

value. Coincidentally, the thresholds recommended by the first three devices were specifically for the measurement of retinal thickness, and that from Spectralis was nonspecific. These findings suggest that the minimum signal quality requirement is closely associated with the type of measurements performed.

The key element in this study was the derivation of the mTCI values, from which we proposed a histogram decomposition model to evaluate OCT images for signal quality. In a similar attempt to evaluate the signal quality for time domain OCT images, Stein et al.[12] developed a quantitative parameter also based on histogram analysis, and reported capability of discriminating time domain OCT images with excellent, acceptable, and poor image quality. Although the methods of subjective and quantitative assessments were different from this report, there was similarity in designing the quantitative parameters. Stein et al.[12] chose the 75th percentile to separate background and foreground, and later the 66th percentile was chosen for spectral domain OCT images (Dr Ishikawa, oral communication, Annual ARVO meeting, 2011). In our histogram model, the N_2 values fall into this range for images with strong signals, because the tissue content for an OCT retinal scan was approximately 600 μm and the axial depth of a scanning window was approximately 2 mm. On the other hand, for OCT images with weak signals, the N_2 values in our histogram model yielded a larger percentage. In comparison, this report extended the OCT histogram modeling and decomposition approach to include analysis of images with weak signals and generalization to OCT devices from multiple manufacturers.

The histogram model was further distilled to three parameters for calculating the mTCI value: the peak intensity (N_1), the separation point between background and foreground (N_2), and the saturation point (N_3) of the histogram. N_1 and N_2 were derived solely from the histogram distribution of the background pixels, and N_3 corresponded to retinal features of the highest intensity, typically pixels in the outer retino-choroid complex. Consequently, mTCI value is unlikely to be affected by the presence of lesions that alter only the retinal structure (e.g., edema, detachment) but without increased reflectance. For highly scattered lesions (e.g., geographical atrophy), the mTCI value is affected only if the reflectance from individual pixels within the lesion complex is significantly higher than those from the outer retino-choroid complex. In this dataset, we did not observe "abnormal" mTCI values with the presence of various retinal lesions.

It was also noted that in this dataset, the distribution of mTCI in Spectralis was different from the other three devices.

Table 3. Recommended MSI Thresholds by Device and the Corresponding SGS and mTCI Values

Device	MSI	SGS	mTCI
Cirrus	6	5.5	5.0
RTVue	39	5.0	4.9
Spectralis	15	5.0	3.1
3D OCT-1000	45	6.4	5.4

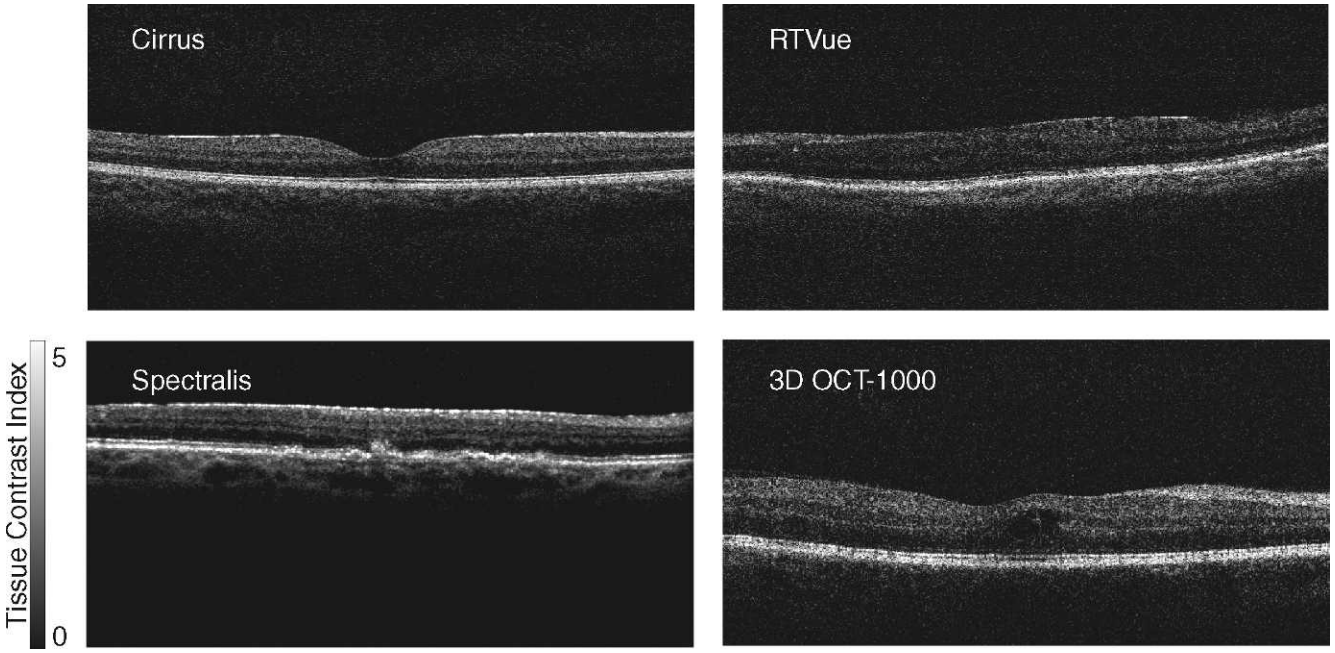

Figure 5. Representative OCT B-scans from four spectral domain-OCT devices were converted using the tissue contrast index, and displayed in the same gray scale. The mTCI measurements of these images are 5.00, 5.12, 4.87, and 4.92, respectively. Pixel intensity was mapped to a range varying from black (TCI = 0) to white (TCI = 5).

The Spectralis data contained a large portion of samples with mTCI value exceeding 8, whereas it was not observed among the other devices in the selected samples. This was because Spectralis data samples were captured with a frame-averaging algorithm (ART = 5). When several frames were averaged, the histogram distribution of the background pixels became narrower (i.e., the intensity difference between N_1 and N_2 became smaller), which caused increased signal-to-noise ratio and mTCI values. When the mTCI algorithm applied to "overlapped" OCT images obtained with instruments other than Spectralis, similar high mTCI values were observed.

It is reasonable to assume that the histogram model is also applicable to other OCT devices; however, caution is warranted, as several factors could affect the accuracy of the model. First, because the model is based on the pixel histogram distribution, it works better with 3-dimensional cube data compared with a single B-scan, especially when a B-scan has limited lateral and axial resolutions. Second, the OCT source data need to be at least 8-bit in precision to minimize the quantization error associated with histogram binning. Last, the model requires adequate detection of the background signals, thus excessive manipulation in the OCT source data, especially arbitrary clipping on the background signal content, will invalidate the model.

Another assumption made in this study is that the interdevice variability in the background histogram characteristics is relatively small for a given device type. This assumption may hold true if the signal detection hardware components in a device were consistently produced; however, for a device with relatively long production history, it is possible that certain modification of the signal detection components occurred during the manufacturing life span. It would be prudent to obtain the noise-profiling image (see Appendix) for each individual device to ensure the consistency in the background histogram characteristics.

Beyond estimating the signal quality of OCT images, the histogram model may also be useful in standardizing display and visualization of OCT images. With the following formula, the OCT image can be linearly transformed into the Tissue Contrast Index (TCI) space,

$$TCI = (I - N_1)/(N_2 - N_1)$$

Where I is the intensity of each OCT pixel, and N_1 and N_2 are calculated based on the method detailed in Appendix A. This allows OCT images from different devices to be comparable in the same metric space and be applied with the same gray scale or pseudo color presentation (e.g., Fig. 5).

In summary, a histogram decomposition model of OCT images was presented, and subjective and objective assessments of the signal quality of OCT images were developed. Strong correlations were found between subjective and objective parameters, and with the signal indices provided by various OCT manufacturers. The methods will be useful in multicenter clinical studies when standardization of OCT images and measurement from different devices is necessary.

Acknowledgments

The authors thank Dr Jeong Won Pak, Charles Chandler, and Thomas W. Pauli for grading OCT images. The authors thank device manufacturers for providing export capability of extracting OCT raw data, which made this study possible.

References

1. Fujimoto J, Bouma B, Tearney G, et al. New technology for high speed and high resolution optical coherence tomography. *Ann N Y Acad Sci*. 1998;838:95–107.
2. van Velthoven ME, Faber DJ, Verbraak FD, van Leeuwen TG, de Smet MD. Recent developments in optical coherence tomography for imaging the retina. *Prog Retin Eye Res*. 2007;26:57–77.
3. Giani A, Cigada M, Choudhry N, et al. Reproducibility of retinal thickness measurements on normal and pathologic eyes by different optical coherence tomography instruments. *Am J Ophthalmol*. 2010;150:815–824.

4. Geitzenauer W, Kiss C, Durbin M, et al. Comparing retinal thickness measurements from cirrus spectral domain-and stratus time domain-optical coherence tomography. *Retina*. 2010;30:596–606.
5. Cheung CYL, Leung CKS, Lin D, Pang CP, Lam DSC. Relationship between retinal nerve fiber layer measurement and signal strength in optical coherence tomography. *Ophthalmology*. 2008;115:1347–1351.
6. Samarawickrama C, Pai A, Huynh SC, Burlutsky G, Wong TY, Mitchell P. Influence of OCT signal strength on macular, optic nerve head, and retinal nerve fiber layer parameters. *Invest Ophthalmol Vis Sci*. 2010;51:4471–4475.
7. El-Ashry M, Appaswamy S, Deokule S, Pagliarini S. The effect of phacoemulsification cataract surgery on the measurement of retinal nerve fiber layer thickness using optical coherence tomography. *Curr Eye Res*. 2006;31:409–413.
8. Folio LS, Wollstein G, Ishikawa H, et al. Variation in optical coherence tomography signal quality as an indicator of retinal nerve fibre layer segmentation error. *Br J Ophthalmol*. 2012; 96:514–518.
9. Rao HL, Kumar AU, Babu JG, Kumar A, Senthil S, Garudadri CS. Predictors of normal optic nerve head, retinal nerve fiber layer, and macular parameters measured by spectral domain optical coherence tomography. *Invest Ophthalmol Vis Sci*. 2011;52: 1103–1110.
10. Balasubramanian M, Bowd C, Vizzeri G, Weinreb RN, Zangwill LM. Effect of image quality on tissue thickness measurements obtained with spectral-domain optical coherence tomography. *Opt Express*. 2009;17:4019–4036.
11. Linnet K. Estimation of the linear relationship between the measurements of two methods with proportional errors. *Stat Med*. 1990;9:1463–1473.
12. Stein D, Ishikawa H, Hariprasad R, et al. A new quality assessment parameter for optical coherence tomography. *Br J Ophthalmol*. 2006;90:186–190.

Appendix: Maximum Tissue Contrast Index (mTCI) Histogram Density Modeling and Decomposition

Histogram Density Modeling and Decomposition

The pixels in an OCT image can be classified into two groups: those pertaining to the background and those pertaining to the foreground. The background consists of pixels corresponding to the vitreous and to the area posterior to the tissues, where there is minimal reflectance. The foreground consists of pixels of various retinal tissues. In an OCT image with strong signal, most of the pixels corresponding to the retinal tissues have higher intensity than those of the background. In contrast, in an OCT image with weak signal, some of the pixels corresponding to tissues have reduced intensity and become indistinguishable from the background. In these images, the number of background pixels increases and the number of foreground pixels decreases.

The relative composition of background and foreground contribution to an OCT image is further illustrated in Figure A1. Figure A1A and Figure A1B show schematic drawings of an intensity histogram of an OCT image and its associated cumulative density function (CDF), the cumulative percentile of the intensity distribution. The histogram plot shows a peak (mode of the histogram) located at the low-intensity region corresponding to background pixels, and asymmetric distribution, with more pixels on the right side of the peak, corresponding to the foreground pixels. N_1, N_2, and N_3 and cN_1, cN_2, and cN_3 denote the intensity and cumulative density values of the mode point, the separation point between background and foreground (i.e., when the accumulative density of the background pixels reaches 99%), and the saturation point ($cN_3 = 99.9\%$ of all pixels).

Table A1. The cN^*_{1B} Was Determined for Each Device Using the Respective Noise-Profiling Images

Device	cN^*_{1B}
Cirrus	0.40
RTVue	0.55
Spectralis	0.45
3D OCT-1000	0.50

cN^*_{1B} was the cumulative percentile at the first location where histogram frequency was ≥95% of the peak frequency in the noise-profiling image.

The model further assumed that for a given OCT instrument, although the number of background pixels varies among the captured OCT images because of the difference in signal quality, the statistical pattern in intensity histogram of the background pixels is the same among all images. Therefore, the ratio between cN_1 and cN_2 remains constant. This observation is further illustrated in Figure A1C.

In addition, for a special case when all pixels are background pixels (i.e., in a noise-profiling image), the relationship is expressed as

$$cN_1/cN_2 = cN_{1B}/cN_{2B},$$

where cN_{1B} and cN_{2B} denote the CDF values for the mode and separation points for the noise-profiling images. By definition, $cN_{2B} = 99.9\%$, and cN_{1B} for each device can be determined experimentally. To obtain a noise-profiling image, the users can capture OCT scans with no target in front of the device. When devices prevent the users from saving images with poor quality, they can be obtained from selected B-scan frames where there is no visible tissue signal.

In implementation, for the purpose of more accurate estimation of cN_2, we substituted cN_1 and cN_{1B} with cN^*_1 and cN^*_{1B}. cN^*_1 was defined as the cumulative percentile at the first location where the histogram frequency was greater than or equal to 95% of the peak frequency at N_1, and cN^*_{1B} was the corresponding measurement in the noise-profiling image. The procedure of computing N_1, N_2, and N_3 and *mTCI* is listed as the following:

(1) Determine the histogram mode intensity N_1.
(2) Find the first location where the frequency was greater than or equal to 95% of the peak frequency at N_1; calculate the CDF value cN^*_1 at this location.
(3) Determine cN_2. $cN_2 = cN^*_1$ x 0.999 / cN^*_{1B}. cN^*_{1B} is listed in Table A1.
(4) Determine the intensity of the separation point N_2.
(5) Determine the saturation intensity N_3.
(6) $mTCI = (N_3 - N_1) / (N_2 - N_1)$.

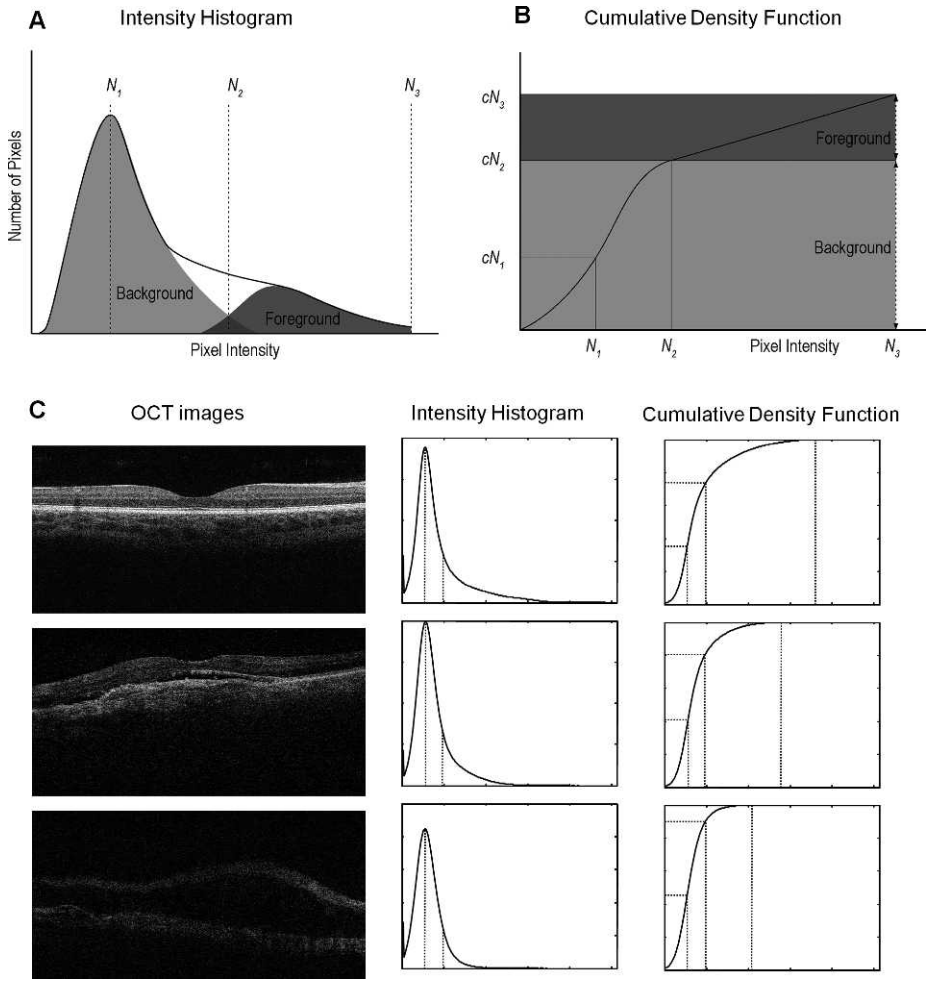

Figure A1. Histogram density modeling and decomposition of an OCT image. (**A**) Schematic drawing of the intensity histogram of an OCT image. Solid line shows the envelope of the histogram, and dotted lines show the relative composition between background and foreground pixels. N_1, N_2, and N_3 denote the signal intensity values of the mode point, the separation point between background and foreground, and the saturation point. (**B**) Schematic drawing of the cumulative density function (CDF) of an OCT image. N_1, N_2, and N_3 and cN_1, cN_2, and cN_3 denote the signal intensity and cumulative density values of the mode point, the separation point between background and foreground, and the saturation point. (**C**) Three representative OCT images with strong, moderate, and weak signals, and their associated intensity histogram and cumulative density functions. The mTCI values of these three images (from strong to weak) are 6.95, 5.55, and 3.50, respectively.